




## Resonant transmission of fermionic carriers: Comparison between solid-state physics and quantum optics approaches

Andrey R. Kolovsky <sup>1,2</sup> and Dmitrii N. Maksimov <sup>1,3</sup>

<sup>1</sup>*Kirensky Institute of Physics, Federal Research Center KSC SB RAS, 660036 Krasnoyarsk, Russia*

<sup>2</sup>*School of Engineering Physics and Radio Electronics, Siberian Federal University, 660041 Krasnoyarsk, Russia*

<sup>3</sup>*IRS SQC, Siberian Federal University, 660041 Krasnoyarsk, Russia*

 (Received 8 April 2021; revised 5 June 2021; accepted 23 August 2021; published 8 September 2021)

We revisit the phenomenon of the resonant transmission of fermionic carriers through a quantum device connected to two contacts with different chemical potentials. We show that, besides the traditional Landauer-Büttiker approach in solid-state physics, this phenomenon can also be described by the non-Markovian master equation for the reduced density matrix of the fermions in the quantum device. We identify validity regions for both approaches in the system parameter space and argue that for large relaxation rates the accuracy of the latter approach greatly exceeds the accuracy of the former.

DOI: [10.1103/PhysRevB.104.115115](https://doi.org/10.1103/PhysRevB.104.115115)

### I. INTRODUCTION

The problem of electron transport in a metallic wire connecting two contacts is older than quantum mechanics [1]. In the past few centuries this problem was readdressed several times, reflecting the progress in experimental physics, where the main milestones are the appearance of clean semiconductors and lithography technology and the emergence of the physics of ultracold atoms. The former technology substituted the wire with an engineered device, a quantum dot [2,3], while with cold atoms in an optical lattice one can mimic the behavior of crystalline electrons in the pure form, i.e., without complications caused by the presence of the long-range Coulomb interaction and electron-phonon interaction [4,5]. These two systems, quantum dots and cold atoms, allow experimentalists to study the coherent transport of carriers (electrons and neutral atoms, respectively) where deviations from the classical Ohm law become especially pronounced.

Concerning the theory, presently, we have a vast array of methods which, however, can be sorted into two large groups. The methods belonging to the first group, which we shall refer to as the solid-state physics approach, are traced back to Landauer's conjecture [6] that the wire conductance is related to the transmission probability, and as a rule, they extensively use the Green's function formalism. The famous result of the solid-state physics approach is the theoretical description of the phenomenon of resonant transmission in quantum dots [7,8]. The methods belonging to the second group, which we shall refer to as the quantum optics approach, operate with very different notions like the quantum master equation for open (generally, many-body) quantum systems and the Born and Markov approximations [9–12]. One can also assign to this group the stochastic methods which explore the correspondence between the master equations and the stochastic Schrödinger equations [13–15]. Remarkably, in spite of the completely different technique the quantum optics approach is also capable of capturing the phenomenon

of resonant transmission [16]. The question arises of how the results of the above two approaches are related to each other and which of them is more accurate. In the present work we answer this question by studying the simple model for quantum transport of fermionic carriers introduced in Refs. [17,18]. This model can be viewed as a modification of the open Hubbard models [19–21], which are representatives of a wider class of the boundary-driven system [22], for which many numerical and analytical results are known [22–25]. The mentioned modification involves the semimicroscopic model for the particle reservoirs [26] that allows one to address the effects which cannot be addressed within the frameworks of the standard open Hubbard models. Alternatively, this model can be viewed as a generalization of the Landauer approach for the electron transport [7,8] in which the relaxation processes in the contacts are explicitly taken into account. Thus, the model can be equally analyzed by using both solid-state physics and quantum optics approaches.

The structure of this paper is as follows. In Sec. II we recall the ingredients of the model and preliminarily discuss the system dynamical regimes depending on the control parameter. Analytical results are collected in Sec. III. This section consists of three subsections in which we employ three different methods to study the system, namely, the Markovian master equation, the non-Markovian master equation, and the Landauer-like approach. In Sec. IV we analyze the coherent properties of the carriers that help us to quantify the degree of validity of these approaches. The main results of the work are summarized in Sec. V.

### II. THE MODEL

We consider a setup consisting of a linear tight-binding chain of length  $L$  coupled at both ends to two tight-binding rings of  $M$  sites each (see Fig. 1 in Ref. [18]). Throughout the text the rings are termed the contacts since they serve as the particle reservoirs. Noninteracting spinless fermions can

hop between the sites of the chain and the sites of the rings with rates  $J_s$  and  $J_r$ , where  $J_s \sim J_r$ , while the hopping between the chain and the contacts is quantified by the coupling constant  $\epsilon \ll J_s, J_r$  [27]. The dynamics is governed by the master equation for the total density matrix

$$\frac{\partial \widehat{\mathcal{R}}}{\partial t} = -i[\widehat{\mathcal{H}}, \widehat{\mathcal{R}}] + \gamma \sum_{\ell=1,L} (\widehat{\mathcal{L}}_{\ell}^{(s)} + \widehat{\mathcal{L}}_{\ell}^{(d)}). \quad (1)$$

In Eq. (1) the Hamiltonian has the form

$$\widehat{\mathcal{H}} = \widehat{\mathcal{H}}_s + \sum_{\ell=1,L} (\widehat{\mathcal{H}}_{r,\ell} + \widehat{\mathcal{H}}_{c,\ell}), \quad (2)$$

where

$$\widehat{\mathcal{H}}_s = -\frac{J_s}{2} \sum_{\ell=1}^{L-1} \hat{c}_{\ell+1}^{\dagger} \hat{c}_{\ell} + \text{H.c.} \quad (3)$$

is the chain Hamiltonian, with  $\hat{c}_{\ell}^{\dagger}$  and  $\hat{c}_{\ell}$  being Fermionic creation and annihilation operators at the  $\ell$ th site. The contact Hamiltonians  $\widehat{\mathcal{H}}_{r,\ell}$  and the coupling Hamiltonians  $\widehat{\mathcal{H}}_{c,\ell}$  are indexed with the subscript  $\ell = 1, L$  specifying the connection site. The contact Hamiltonians are written in terms of Fermionic operators acting in the Fock space of the Bloch eigenstates of the ring,

$$\widehat{\mathcal{H}}_r = -J_r \sum_{k=1}^M \cos\left(\frac{2\pi k}{M}\right) \hat{b}_k^{\dagger} \hat{b}_k \quad (4)$$

(here we dropped the subscript  $\ell$  assuming that the rings are identical). The coupling Hamiltonian is given by

$$\widehat{\mathcal{H}}_{c,\ell} = -\frac{\epsilon}{2\sqrt{M}} \sum_{k=1}^M \hat{c}_{\ell}^{\dagger} \hat{b}_k + \text{H.c.} \quad (5)$$

To prescribe thermodynamic quantities to each contact we introduced the particle drain,

$$\widehat{\mathcal{L}}_{\ell}^{(d)} = \sum_{k=1}^M \frac{\bar{n}_{k,\ell} - 1}{2} (\hat{b}_k^{\dagger} \hat{b}_k \widehat{\mathcal{R}} - 2\hat{b}_k \widehat{\mathcal{R}} \hat{b}_k^{\dagger} + \widehat{\mathcal{R}} \hat{b}_k^{\dagger} \hat{b}_k), \quad (6)$$

and the particle gain,

$$\widehat{\mathcal{L}}_{\ell}^{(s)} = -\sum_{k=1}^M \frac{\bar{n}_{k,\ell}}{2} (\hat{b}_k \hat{b}_k^{\dagger} \widehat{\mathcal{R}} - 2\hat{b}_k^{\dagger} \widehat{\mathcal{R}} \hat{b}_k + \widehat{\mathcal{R}} \hat{b}_k \hat{b}_k^{\dagger}), \quad (7)$$

where

$$\bar{n}_{k,\ell} = \frac{1}{e^{-\beta_{\ell}[J_r \cos(2\pi k/M) + \mu_{\ell}]} + 1}. \quad (8)$$

This ensures that the Bloch states of isolated contacts are populated according to the Fermi-Dirac distribution with a given chemical potential  $\mu_{\ell}$  and inverse temperature  $\beta_{\ell}$ . Finally, the constant  $\gamma$  in Eq. (1) is the relaxation rate which determines how fast the isolated contacts relax to their thermodynamic equilibrium. It was shown in Ref. [18] that the considered model validates the main assumption of the Landauer approach about the reflectionless contacts, thus allowing for the straightforward application of this theory.

Unlike Ref. [18], in the present work we shall consider a short chain with which one can observe the phenomenon of

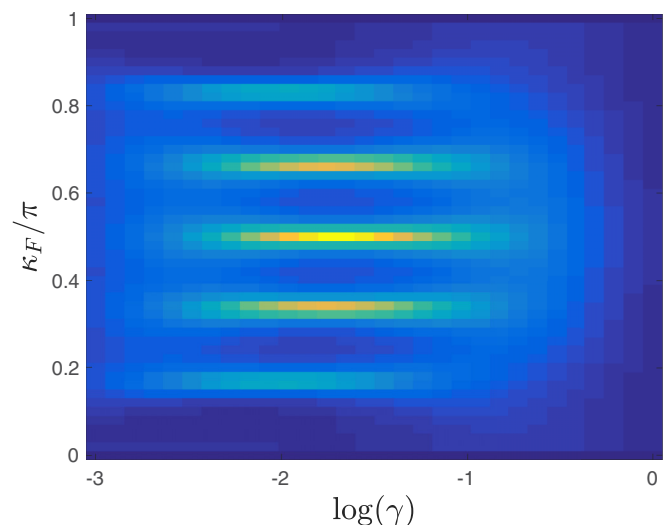


FIG. 1. The current across the tight-binding chain of length  $L = 5$  as a function of  $\kappa_F$  and the relaxation constant  $\gamma$ . The hopping matrix elements are  $J_s = J_r = 1$ , the coupling constant  $\epsilon = 0.4$ , the temperature  $1/\beta = 0$ , the size of the rings  $M = 100$ , and the difference in the contact chemical potentials  $\Delta\mu = J_r \sin(\kappa_F)(2\pi/M)$ .

resonant transmission. Also we focus on the linear response regime where the current across the chain is proportional to the contact chemical potential difference. As an example, Figs. 1 and 2 show the results of the numerical analysis of the model for  $\beta = \infty$ ,  $L = 5$ , and  $M = 100$ , which is large enough to speak about the quasicontinuous spectrum of the contacts [28]. In these numerical simulations we evolve the system in time until the density matrix  $\mathcal{R}(t)$  reaches its stationary value from which we determine the stationary cur-

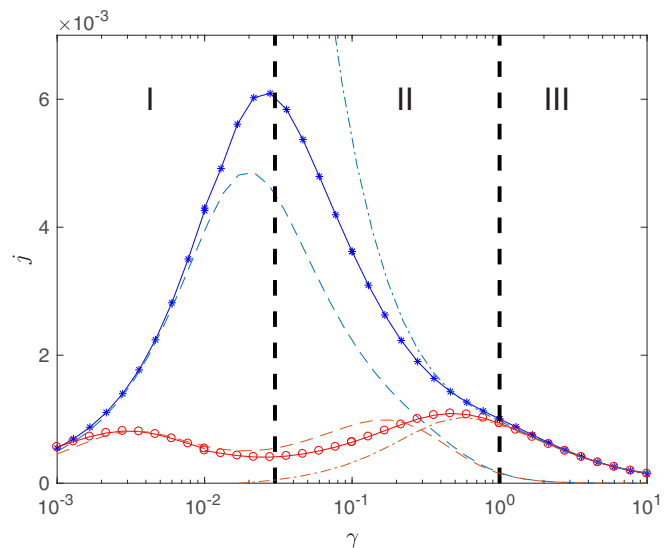


FIG. 2. The current as a function of the relaxation constant  $\gamma$  for  $\kappa_F = \pi/2$  ( $\mu = 0$ ; blue asterisks) and  $\kappa_F \approx 0.58\pi$  (red circles). Vertical dashed lines demark different dynamical regimes of the system with respect to the Born and Markov approximations. The additional dashed and dash-dotted lines are results of the algebraic approaches (see the text).

rent  $j$ . In Fig. 1 we depict the stationary current as a color map where the phenomenon of the resonant transmission is seen as local peaks at the values of the chemical potential  $\mu = -J_r \cos(\kappa_F)$  coinciding with eigenenergies of the isolated tight-binding chain. Notice that the peaks are present only in a certain interval of  $\gamma$ . Figure 2 shows the current as a function of  $\gamma$  for  $\mu = 0$  (the central peak in Fig. 1) and  $\mu = 0.25$  (the nearby deep). Figure 2 is aimed at illustrating the Esaki-Tsu-like dependence [29–32] of the current on the relaxation rate  $\gamma$ , with the universal asymptotic  $j \sim \gamma$  for  $\gamma \rightarrow 0$  and  $j \sim 1/\gamma$  for  $\gamma \rightarrow \infty$ . In Fig. 2 we also demark by the vertical dashed lines the different dynamical regimes of the system which we briefly discuss in the next paragraph.

In parameter region III the large value of the relaxation constant  $\gamma$  validates the Born and Markov approximations for the carriers in the chain that allow us to derive the Markovian master equation for the reduced density matrix of the carriers in the chain (see Sec. III C). In region II the Markov approximation fails; however, the Born approximation is still valid. In the other words, the ergodic properties of the contacts, when they are viewed as particle reservoirs, are not affected by the presence of the chain. The direct consequence of this fact is that the reduced density matrices of the contacts remain close to their thermodynamic equilibrium [33]. The failure of the Markov approximation leads to the non-Markovian (integro-differential) master equation for the reduced density matrix of the carriers in the chain (see Sec. III B). Finally, if we move to region I we break both the Markov and Born approximations. To analyze the system in this region we employ the solid-state physics approach. Section III A shows that this approach gives quantitatively correct results in region I and qualitatively correct results in region II. However, it fails to reproduce the case of large  $\gamma$  for which it gives the wrong asymptotic  $j \sim 1/\gamma^2$ .

### III. QUANTUM TRANSPORT ACROSS THE TIGHT-BINDING CHAIN

Equation (1) contains only pairwise combinations of the creation and annihilation operators. This allows us to rewrite it in terms of the single-particle density matrix (SPDM)  $\hat{\rho}$ . Let us assume for a moment that only one (the left) contact is attached to the chain. Then the total SPDM takes the following block form:

$$\hat{\rho} = \begin{pmatrix} \hat{\rho}_r & \hat{\rho}_c \\ \hat{\rho}_c^\dagger & \hat{\rho}_s \end{pmatrix}, \quad (9)$$

where  $\hat{\rho}_r$  is the SPDM of the contact with the elements  $\rho_{k,k'} = \text{Tr}(\hat{b}_k^\dagger \hat{b}_{k'} \hat{\mathcal{R}})$ ,  $\hat{\rho}_s$  is the SPDM of the chain with the elements  $\rho_{\ell,\ell'} = \text{Tr}(\hat{c}_\ell^\dagger \hat{c}_{\ell'} \hat{\mathcal{R}})$ , and  $\hat{\rho}_c$  has the elements  $\rho_{k,\ell} = \text{Tr}(\hat{b}_k^\dagger \hat{c}_\ell \hat{\mathcal{R}})$ . It can be shown from Eq. (1) that the introduced SPDMs obey the following system of three coupled equations:

$$\frac{\partial \hat{\rho}_s}{\partial t} = -i[\hat{H}_s, \hat{\rho}_s] - i\epsilon(\hat{V}_1^\dagger \hat{\rho}_c - \hat{\rho}_c^\dagger \hat{V}_1), \quad (10)$$

$$\frac{\partial \hat{\rho}_c}{\partial t} = -i\hat{H}_r \hat{\rho}_c + i\hat{\rho}_c \hat{H}_s - \frac{\gamma}{2} \hat{\rho}_c - i\epsilon(\hat{V}_1 \hat{\rho}_s - \hat{\rho}_r \hat{V}_1), \quad (11)$$

$$\frac{\partial \hat{\rho}_r}{\partial t} = -i[\hat{H}_r, \hat{\rho}_r] - i\epsilon(\hat{V}_1 \hat{\rho}_c^\dagger - \hat{\rho}_c \hat{V}_1^\dagger) + \gamma(\hat{\rho}_r^{(0)} - \hat{\rho}_r), \quad (12)$$

where  $\hat{H}_s$  is the single-particle Hamiltonian of the chain,

$$\hat{H}_s = -\frac{J_s}{2} \sum_{\ell=1}^{L-1} (|1+\ell\rangle\langle\ell| + \text{H.c.}), \quad (13)$$

$\hat{H}_r$  is the single-particle Hamiltonian of the contact,

$$\hat{H}_r = -J_r \sum_{k=1}^M \cos\left(\frac{2\pi k}{M}\right) |k\rangle\langle k|, \quad (14)$$

$\hat{V}_1$  is the coupling operator,

$$\hat{V}_1 = \frac{1}{2\sqrt{M}} \sum_{k=1}^M |k\rangle\langle\ell=1|, \quad (15)$$

and  $\hat{\rho}_r^{(0)}$  is the thermal SPDM of the carriers in the contact,

$$\hat{\rho}_r^{(0)} = \sum_{k=1}^M \frac{|k\rangle\langle k|}{e^{-\beta[J_r \cos(2\pi k/M) + \mu]} + 1}. \quad (16)$$

This set of equations can be easily generalized to the case of two contacts in which the second contact is attached to last site of the chain. When treating the latter case, we shall change notation for the contact SPDM from  $\hat{\rho}_r$  to  $\hat{\rho}_\ell$ , where  $\ell$  takes the value  $\ell = 1$  for the left contact and  $\ell = L$  for the right contact.

#### A. The limit of small $\gamma$

Let us approximate Eqs. (10)–(12) by a single equation of the form

$$\frac{\partial \hat{\rho}}{\partial t} = -i[\hat{H}, \hat{\rho}] - \gamma(\hat{\rho} - \hat{\rho}_0), \quad (17)$$

where  $\hat{\rho}_0 = \hat{\rho}_r^{(0)} \oplus \hat{0}_s$  ( $\hat{0}_s$  is the zero matrix of size  $L \times L$ ) and  $\hat{H}$  is the total Hamiltonian,

$$\hat{H} = \begin{pmatrix} \hat{H}_r & \epsilon \hat{V}_1 \\ \epsilon \hat{V}_1^\dagger & \hat{H}_s \end{pmatrix}. \quad (18)$$

This approximation is valid in the limit  $\gamma \rightarrow 0$  for the asymptotically large time where the matrix  $\hat{\rho}$  is close to its stationary value. Notice that the limit  $\gamma \rightarrow 0$  implies that the system (18) relaxes to its stationary value as a whole, and hence, there is no way to obtain the equation for  $\hat{\rho}_s$  in the closed form.

The introduced Eq. (17) can be solved analytically by using the eigenstates  $|\Psi_n\rangle$ ,

$$\hat{H}|\Psi_n\rangle = \mathcal{E}_n|\Psi_n\rangle, \quad (19)$$

of the total Hamiltonian (18). In particular, the stationary total density matrix is given by the equation [32]

$$\hat{\rho} = \sum_{n,m} \frac{\gamma \langle \Psi_n | \hat{\rho}_0 | \Psi_m \rangle}{\gamma + i(\mathcal{E}_m - \mathcal{E}_n)} |\Psi_n\rangle\langle \Psi_m|. \quad (20)$$

In the case of two contacts this equation determines the stationary current across the chain through the relation

$$j = \sum_{p>0} \sum_n \frac{\gamma \langle \Psi_n | \hat{\rho}_0 | \Psi_{n+p} \rangle}{\gamma + i(\mathcal{E}_{n+p} - \mathcal{E}_n)} \langle \Psi_{n+p} | \hat{j} | \Psi_n \rangle, \quad (21)$$

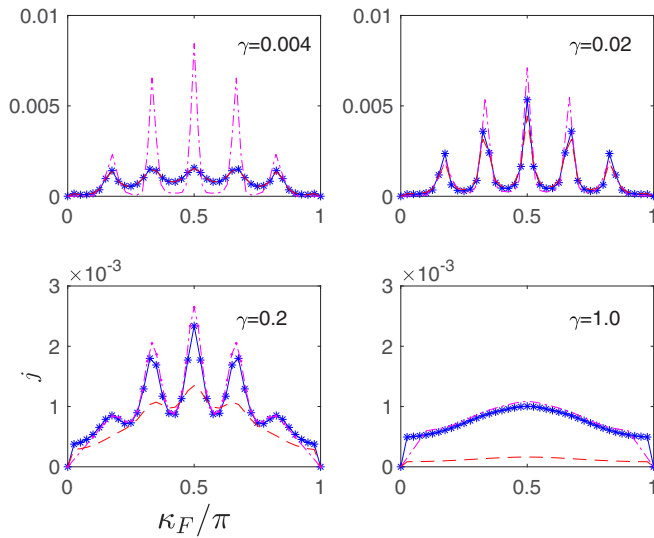


FIG. 3. Comparison of the stationary current calculated on the basis of Eq. (21), (dashed red lines) and on the basis of Eq. (37), (dash-dotted magenta lines), with the result obtained on the basis of the original model (blue symbols).

where  $|\psi_n\rangle$  is the part of the total wave function  $|\Psi_n\rangle$  which resides in the chain and  $\hat{j}$  is the current operator,

$$\hat{j} = -\frac{J_s}{2i} \frac{1}{L-1} \sum_{\ell=1}^{L-1} (|\ell+1\rangle\langle\ell| - \text{H.c.}). \quad (22)$$

In Fig. 3 we compare the stationary current calculated on the basis of the original master equation with that obtained on the basis of Eq. (21). Good agreement for small  $\gamma \leq 0.02$  is noticed.

Equation (21) also provides a simple explanation for the observed resonant structure of the current. In fact, this structure is already reproduced if we keep in Eq. (21) only one term with  $p=1$ . (The term with  $p=0$  vanishes due to the wave function symmetry.) Thus, the transmission peaks are due to the property of the current matrix elements which we shall characterize by the function

$$j(E) = \sum_n \delta(E - \mathcal{E}_n) \langle \psi_n | \hat{j} | \psi_{n+1} \rangle. \quad (23)$$

By definition, function (23) is close to the local density of states (LDS),

$$\text{LDS} = \sum_n \delta(E - \mathcal{E}_n) \langle \psi_n | \psi_n \rangle, \quad (24)$$

which lies behind the concept of the level broadening in the solid-state physics approach and which is directly related to the transmission probability  $|t(E)|^2$ . For the parameters in Fig. 3 the function  $j(E)$  and the local density of states are plotted in Fig. 4. In principle, by using the Green's function one can extend the analysis of Eq. (21) further [7]; however, this goes beyond our aim, which is to identify the validity regions of the different approaches. It is seen in Fig. 3 (see also the dashed lines in Fig. 2) that the approach based on the scattering theory underestimates the current for large  $\gamma$ .

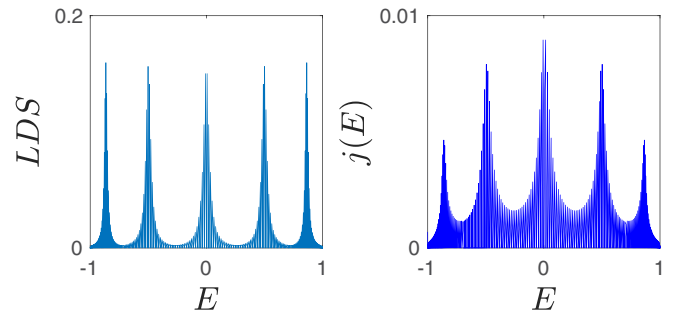


FIG. 4. The chain local density of states (left panel) and function (23) (right panel).

## B. Non-Markovian master equation

In this section we discuss the quantum optics approach based on the non-Markovian master equation for the carriers in the chain. We briefly come back to Eqs. (10)–(12), which refer to the case of the single contact. From Eq. (11) we find the formal solution with the initial condition  $\hat{\rho}_c(0) = 0$ ,

$$\hat{\rho}_c = i\epsilon \int_0^t d\tau e^{\frac{\gamma}{2}(\tau-t)} \hat{U}_r^\dagger(t-\tau) [\hat{\rho}_r(\tau) \hat{V}_1 - \hat{V}_1 \hat{\rho}_s(\tau)] \hat{U}_s(t-\tau), \quad (25)$$

where  $\hat{U}_{s,r}(t) = \widehat{\text{exp}}(-i\hat{H}_{s,r}t)$  are the evolution operators. Employing the Born approximation, i.e., substituting  $\hat{\rho}_r(\tau)$  by  $\hat{\rho}_r^{(0)}$  in Eq. (25) and then substituting this equation into Eq. (10), one obtains the non-Markovian master equation for the carriers in the chain,

$$\frac{\partial \hat{\rho}_s}{\partial t} = -i[\hat{H}_s, \hat{\rho}_s] + \epsilon^2 (\hat{L}_1 + \hat{L}_1^\dagger), \quad (26)$$

where

$$\hat{L}_1 = \int_{-t}^0 d\tau e^{\frac{\gamma}{2}\tau} \hat{V}_1^\dagger \hat{U}_r^\dagger(\tau) [\hat{\rho}_r^{(0)} \hat{V}_1 - \hat{V}_1 \hat{\rho}_s(\tau+t)] \hat{U}_s(\tau) \quad (27)$$

and, to stress the memory effect, we change the integration limits. Next, by taking the limit  $M \rightarrow \infty$  we obtain

$$\hat{L}_1 = \frac{|1\rangle\langle 1|}{4} \int_{-t}^0 d\tau e^{\frac{\gamma}{2}\tau} [\mathcal{J}_F(J_r\tau) \hat{\mathbb{I}}_s - \mathcal{J}_0(J_r\tau) \hat{\rho}_s(\tau+t)] \hat{U}_s(\tau), \quad (28)$$

where  $\mathcal{J}_0$  is the zeroth-order Bessel function of the first kind,  $\hat{\mathbb{I}}_s$  is the identity matrix of size  $L \times L$ , and

$$\mathcal{J}_F(J_r t) = \frac{1}{2\pi} \int_{-\pi}^{\pi} d\kappa \frac{e^{-iJ_r \cos(\kappa)t}}{e^{-\beta[J_r \cos(\kappa) + \mu]} + 1}. \quad (29)$$

In the case of two contacts the above procedure results in the equation

$$\frac{\partial \hat{\rho}_s}{\partial t} = -i[\hat{H}_s, \hat{\rho}_s] + \epsilon^2 \sum_{\ell=1,L} (\hat{L}_\ell + \hat{L}_\ell^\dagger), \quad (30)$$

where the operator  $\hat{L}_L$  has a form similar to Eq. (28) with the projection operator  $|1\rangle\langle 1|$  substituted by  $|L\rangle\langle L|$  and a generally different value of the chemical potential in Eq. (29). Equation (30) together with Eq. (28) constitutes the non-Markovian master equation for the fermionic transport [34]. Notice the key role of  $\gamma$  in Eq. (28)—since the Bessel function at large  $t$  decays as  $1/\sqrt{t}$ , the integral in Eq. (28) is convergent only with nonzero  $\gamma$ .

To check the obtained non-Markovian master equation we solve it numerically and compare the result with that obtained on the basis of the original master equation where we do not take the limit  $M \rightarrow \infty$  and do not *a priori* assume the validity of the Born approximation. It is seen in Fig. 3 that the non-Markovian master equation well reproduces the resonant structure for the stationary current with nice quantitative agreement in regions II and III.

The obtained master equation can be elaborated further if  $\Delta\mu \ll \mu$  and one considers the low-temperature limit  $\beta \rightarrow \infty$ . The former condition justifies the ansatz

$$\hat{\rho}_s = \hat{\rho}_s^{(0)} + \Delta\mu \hat{\rho}_s^{(1)}, \quad (31)$$

where  $\hat{\rho}_s^{(0)}$  is the equilibrium density matrix for  $\Delta\mu = 0$ , which does not support the directed current. The latter condition justifies the relation

$$\lim_{\beta \rightarrow \infty} n(E, \mu + \Delta\mu) = \theta(\mu - E) + \Delta\mu \delta(E - \mu), \quad (32)$$

where  $\theta$  is the Heaviside function. Using these approximations, one finds from Eq. (30)

$$\frac{\partial \hat{\rho}_s^{(1)}}{\partial t} = -i[\hat{H}_s, \hat{\rho}_s^{(1)}] + \epsilon^2 \sum_{\ell=1,L} (\hat{\Delta}_\ell + \hat{\Delta}_\ell^\dagger), \quad (33)$$

where

$$\begin{aligned} \hat{\Delta}_\ell &= \frac{|\ell\rangle\langle\ell|}{4} \int_{-t}^0 d\tau e^{\frac{\gamma}{2}\tau} [d(\mu) \delta_1^\ell e^{i\mu\tau} \hat{\mathbb{I}}_s \\ &\quad - \mathcal{J}_0(J_r \tau) \hat{\rho}_s^{(1)}(\tau + t)] \hat{U}_s(\tau), \end{aligned} \quad (34)$$

with  $d(\mu)$  being the contact density of states,

$$d(\mu) = \begin{cases} \frac{J_r}{\pi \sqrt{J_r^2 - \mu^2}} & \text{if } |J_r| > |\mu|, \\ 0 & \text{if } |J_r| < |\mu|. \end{cases} \quad (35)$$

Finally, from Eq. (33) we obtain the algebraic equation for the stationary  $\hat{\rho}_s^{(1)}$ . In the chain eigenbasis  $|\Phi_n\rangle$ ,

$$\hat{H}_s |\Phi_n\rangle = E_n |\Phi_n\rangle, \quad (36)$$

it reads

$$i[H_s, \hat{\rho}_s^{(1)}] + \frac{\epsilon^2}{4} [(C_1 + C_L) \hat{\rho}_s^{(1)} B + \text{H.c.}] = \frac{\epsilon^2}{4} (C_1 A + \text{H.c.}), \quad (37)$$

where  $H_s$  is the diagonal matrix of the eigenvalues  $E_n$ ,  $B$  is the diagonal matrix with the elements

$$B_{n,n} = \frac{1}{\sqrt{J_r^2 - (E_n + i\gamma/2)^2}}, \quad (38)$$

$A$  is the diagonal matrix with the elements

$$A_{n,n} = \frac{d(\mu)}{\gamma/2 + i(\mu - E_n)}, \quad (39)$$

and  $C_1$  and  $C_L$  are determined by the eigenmodes of the isolated chain,

$$C_{n,m} = \langle \Phi_n | \ell \rangle \langle \ell | \Phi_m \rangle, \quad \ell = 1, L. \quad (40)$$

It follows from Eq. (37) that the matrix  $\hat{\rho}_s^{(1)}$  (which is proportional to the right-hand side of the equation) crucially depends on the value of the chemical potential due to the resonancelike dependence of the matrix  $A$  on the chemical potential  $\mu$ .

The advantage of the discussed algebraic approach (as well as the algebraic approach in Sec. III A) is that it allows us to predict the stationary current without simulating the system dynamics, which reduces the computational time by orders of magnitude. For large  $\gamma$  the predictions based on Eq. (37) are plotted in Fig. 2 by the dash-dotted lines. Taking into account that Eq. (37) involves even more approximations than the non-Markovian master equation (30), the agreement with the results of the straightforward numerical simulation of the system dynamics is quite satisfactory.

### C. Markovian master equation

The Markov approximation assumes that one can neglect the memory effects. It is justified if  $\hat{\rho}_s(t)$  is a slowly varying matrix in the timescale  $1/\gamma$ . Then, by using the general relation for the slowly varying function,

$$\int_0^t d\tau e^{\frac{\gamma}{2}\tau} \mathcal{A}(\tau + t) = \frac{2}{\gamma} \mathcal{A}(t), \quad (41)$$

Eq. (28) simplifies to

$$\hat{L}_\ell = \frac{|\ell\rangle\langle\ell|}{2\gamma} [\bar{n}_\ell \hat{\mathbb{I}}_s - \hat{\rho}_s(t)], \quad (42)$$

where we take into account that  $\mathcal{J}(0) = 1$  while  $\mathcal{J}_F(0)$  equals the mean occupation number  $\bar{n}_\ell$  of the ring sites according to Eq. (29). Substituting Eq. (42) into Eq. (30), we obtain

$$\frac{\partial \hat{\rho}_s}{\partial t} = -i[\hat{H}_s, \hat{\rho}_s] - \tilde{\gamma} \sum_{\ell=1,L} \left( \frac{1}{2} \{|\ell\rangle\langle\ell|, \hat{\rho}_s\} - \bar{n}_\ell |\ell\rangle\langle\ell| \right), \quad (43)$$

where

$$\tilde{\gamma} = \frac{\epsilon^2}{\gamma}. \quad (44)$$

It follows from Eq. (43) that the characteristic timescale for  $\hat{\rho}_s(t)$  is determined by the inverse effective relaxation constant  $1/\tilde{\gamma}$ . Thus, the Markov approximation requires  $\gamma \gg \epsilon$ .

The obtained Markovian master equation (43) coincides with the equation for SPDM of the open Fermi-Hubbard model, which in the case of spinless Fermions reads

$$\frac{\partial \hat{\mathcal{R}}_s}{\partial t} = -i[\hat{\mathcal{H}}_s, \hat{\mathcal{R}}_s] + \tilde{\gamma} \sum_{\ell=1,L} (\hat{\mathcal{L}}_\ell^{(g)} + \hat{\mathcal{L}}_\ell^{(d)}), \quad (45)$$

where  $\hat{\mathcal{H}}_s$  is given in Eq. (3) and the drain and gain Lindblad operators acting on the edge sites of the chain have the form

$$\hat{\mathcal{L}}_\ell^{(d)} = \frac{\bar{n}_\ell - 1}{2} (\hat{c}_\ell \hat{c}_\ell^\dagger \hat{\mathcal{R}} - 2\hat{c}_\ell^\dagger \hat{\mathcal{R}} \hat{c}_\ell + \hat{\mathcal{R}} \hat{c}_\ell \hat{c}_\ell^\dagger) \quad (46)$$

and

$$\hat{\mathcal{L}}_\ell^{(g)} = -\frac{\bar{n}_\ell}{2} (\hat{c}_\ell \hat{c}_\ell^\dagger \hat{\mathcal{R}} - 2\hat{c}_\ell^\dagger \hat{\mathcal{R}} \hat{c}_\ell + \hat{\mathcal{R}} \hat{c}_\ell \hat{c}_\ell^\dagger). \quad (47)$$

The open Fermi-Hubbard model was analyzed earlier in Ref. [35] with the following result for the mean current:

$$j = \frac{J_s^2 \tilde{\gamma}}{J_s^2 + \tilde{\gamma}^2} \frac{\bar{n}_1 - \bar{n}_L}{2}. \quad (48)$$

Since Eq. (48) involves only the mean density of carriers in the contacts, it approximates the exact results only in the



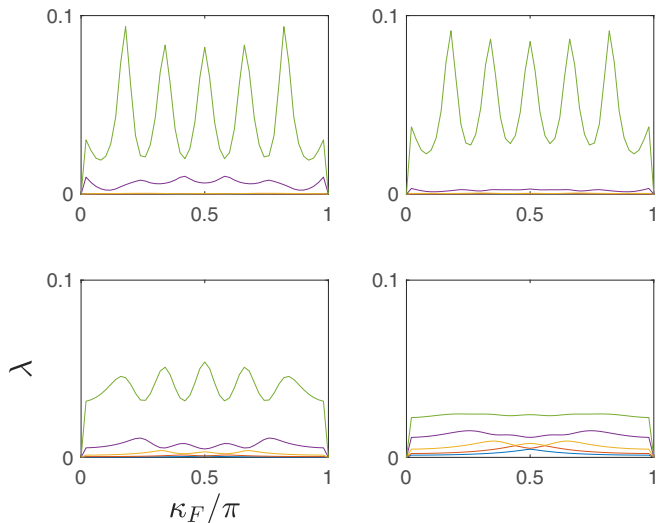


FIG. 5. Eigenvalues of stationary matrix  $\hat{\rho}_s^{(1)}$  as a function of  $\kappa_F$ . The system parameters are the same as in Fig. 3.

limit  $\gamma \rightarrow \infty$  where the stationary current does not show any resonant structure.

#### IV. COHERENCE OF THE TRANSPORTING STATES

At the end of Sec. III A we introduced the density matrix  $\hat{\rho}_s^{(1)}$  which characterizes the stationary current across the chain in the linear response regime (i.e., determines the conductance). In what follows we shall term this matrix the transporting state. It is interesting to address the question of how close the transporting state is to a pure state. In Fig. 5 we plot eigenvalues of  $\hat{\rho}_s^{(1)}$  for four different values of the relaxation constant  $\gamma$  which we used in Fig. 3. By comparing Figs. 5 and 3 we conclude that the transporting state is close to a pure state (which has to have a single nonzero eigenvalue) only in the interval of  $\gamma$  where the stationary current shows the resonant structure. Moreover, even for these  $\gamma$  the coherence of the transporting state depends on the value of the chemical potential  $\mu$ . Namely, the state is more coherent for  $\mu$  corresponding to the transmission peaks and essentially less coherent for  $\mu$  corresponding to the transmission deeps. This result stresses the main difference of the discussed master equation approach from the Landauer-like approaches which

implicitly assume that the transport state of the fermionic carriers in the chain is the pure state given by the Bloch wave with the Fermi quasimomentum.

#### V. CONCLUSION

We revisited the problem of the quantum transport of fermionic particles across a tight-binding chain connected to two contacts. The analysis was performed by using the simple model introduced in our earlier work [18] in which the contacts are modeled by tight-binding rings of arbitrary size. The coupling between the chain and contacts is controlled by the parameter  $\epsilon$ , and the contacts are characterized by their chemical potentials  $\mu$  and the temperature  $1/\beta$ . The mathematical framework of the model is the master equation for the total density matrix of the composed system chain plus contacts which involves the important physical parameter  $\gamma$ , the rate at which the isolated contacts relax to thermodynamic equilibrium. Although in reality the rate  $\gamma$  correlates with the contact temperature (indeed, it looks unfeasible to have low rates at high temperatures and vice versa), in this work we considered  $\gamma$  and  $\beta$  independent parameters.

We calculated the current in the chain by using three different approaches: the Markovian and non-Markovian master equations for the reduced density matrix of the carriers in the chain and the Landauer-like approach for the quantum transport. We discussed in detail each of the listed approaches and identified the regions of their validity. In particular, it was found that the non-Markovian master equation approach (which is representative of quantum optics approaches) and the Landauer approach (which is representative of the solid-state physics approaches) do reproduce the resonant structure of the stationary current. However, the former approach overestimates it in the region of small  $\gamma$ , while the latter approach underestimates the current in the region of large  $\gamma$ . For moderate  $\gamma$ , where oscillations of the stationary current  $j = j(\mu)$  have maximal amplitude, both the solid-state physics and quantum optics approaches give essentially the same result.

#### ACKNOWLEDGMENTS

We acknowledge financial support from the Russian Science Foundation through Grant No. 19-12-00167.

- 
- [1] G. S. Ohm, *Die Galvanische Kette: Mathematisch Bearbeitet* (Riemann, Berlin, 1827).
  - [2] M. A. Kastner, Artificial atoms, *Phys. Today* **46**(1), 24 (1993).
  - [3] R. C. Ashoori, Electrons in artificial atoms, *Nature (London)* **379**, 413 (1996).
  - [4] B. T. Seaman, M. Krämer, D. Z. Anderson, and M. J. Holland, Atomtronics: Ultracold-atom analogs of electronic devices, *Phys. Rev. A* **75**, 023615 (2007).
  - [5] I. Bloch, J. Dalibard, and S. Nascimbéne, Quantum simulations with ultracold quantum gases, *Nat. Phys.* **8**, 267 (2012).
  - [6] R. Landauer, Conductance from transmission: Common sense points, *Phys. Scr.* **T42**, 110 (1992).
  - [7] S. Datta, *Electronic Transport in Mesoscopic Systems* (Cambridge University Press, Cambridge, 1995).
  - [8] S. Datta, *Quantum Transport: Atom to Transistor* (Cambridge University Press, Cambridge, 2005).
  - [9] E. B. Davies, *Quantum Theory of Open Systems* (Academic, London, 1976).
  - [10] H.-P. Breuer and F. Petruccione, *The Theory of Open Quantum Systems* (Oxford University Press, New York, 2007).
  - [11] A. R. Kolovsky, Quantum entanglement and the Born-Markov approximation for an open quantum system, *Phys. Rev. E* **101**, 062116 (2020).

- [12] P. B. Vyas, M. L. Van de Put, and M. V. Fischetti, Master-equation Study of Quantum Transport in Realistic Semiconductor Devices Including Electron-Phonon and Surface-Roughness Scattering, *Phys. Rev. Appl.* **13**, 014067 (2020).
- [13] L. Diósi, N. Gisin, and W. T. Strunz, Non-Markovian quantum state diffusion, *Phys. Rev. A* **58**, 1699 (1998).
- [14] X. Zhao, W. Shi, L.-A. Wu, and T. Yu, Fermionic stochastic Schrödinger equation and master equation: An open-system model, *Phys. Rev. A* **86**, 032116 (2012).
- [15] M. Chen and J. Q. You, Non-Markovian quantum state diffusion for an open quantum system in fermionic environments, *Phys. Rev. A* **87**, 052108 (2013).
- [16] A. R. Kolovsky and D. N. Maksimov, Non-Markovian master equation for quantum transport of fermionic carriers (unpublished).
- [17] S. Ajisaka, F. Barra, C. Mejía-Monasterio, and T. Prosen, Nonequilibrium particle and energy currents in quantum chains connected to mesoscopic Fermi reservoirs, *Phys. Rev. B* **86**, 125111 (2012).
- [18] A. R. Kolovsky, Open Fermi-Hubbard model: Landauer's versus master equation approaches, *Phys. Rev. B* **102**, 174310 (2020).
- [19] T. Prosen, Exact Non-equilibrium Steady State of an Open Hubbard Chain, *Phys. Rev. Lett.* **112**, 030603 (2014).
- [20] A. Ivanov, G. Kordas, A. Komnik, and S. Wimberger, Bosonic transport through a chain of quantum dots, *Eur. Phys. J. B* **86**, 345 (2013).
- [21] A. R. Kolovsky, Z. Denis, and S. Wimberger, Landauer-Büttiker equation for bosonic carriers, *Phys. Rev. A* **98**, 043623 (2018).
- [22] G. T. Landi, D. Poletti, and G. Schaller, Non-equilibrium boundary driven quantum systems: Models, methods and properties, [arXiv:2104.14350](https://arxiv.org/abs/2104.14350).
- [23] Y. Dubi and M. Di Ventra, Fourier's law: Insight from a simple derivation, *Phys. Rev. E* **79**, 042101 (2009).
- [24] M. Žnidarič, Exact solution for a diffusive nonequilibrium steady state of an open quantum chain, *J. Stat. Mech.* (2010) L05002.
- [25] A. Asadian, D. Manzano, M. Tiersch, and H. J. Briegel, Heat transport through lattices of quantum harmonic oscillators in arbitrary dimensions, *Phys. Rev. E* **87**, 012109 (2013).
- [26] Here the term "semimicroscopic" is used to distinguish it from the fully microscopic models of the particle reservoirs [36].
- [27] Formally, the smaller  $\epsilon$  is, the better the agreement between analytical and numerical results is expected to be. However, since the actual parameter which quantifies the effect of the contacts is  $\epsilon^2$ , not  $\epsilon$  (see the equations for the reduced density matrix in Secs. III B and III C), we have good agreement even for  $\epsilon = 0.4$  used in Fig. 1. From the viewpoint of numerical simulations of the system dynamics large  $\epsilon$  is preferable because it reduces the relaxation time to the steady-state regime.
- [28] This statement can be quantified by studying the convergence of Eq. (28) where the integral over  $\kappa$  in Eq. (29) is substituted by the sum over discrete  $\kappa = 2\pi k/M$ . Notice that the larger  $\gamma$  is, the faster the convergence is.
- [29] L. Esaki and R. Tsu, Superlattice and negative differential conductivity in semiconductors, *IBM J. Res. Develop.* **14**, 61 (1970).
- [30] C. Minot, Quantum model of electronic transport in superlattice minibands, *Phys. Rev. B* **70**, 161309(R) (2004).
- [31] H. Ott, E. de Mirandes, F. Ferlaino, G. Roati, G. Modugno, and M. Inguscio, Collisionally Induced Transport in Periodic Potentials, *Phys. Rev. Lett.* **92**, 160601 (2004).
- [32] A. R. Kolovsky, Atomic current in optical lattices: Reexamination of the Esaki-Tsu equation, *Phys. Rev. A* **77**, 063604 (2008).
- [33] We mention that this statement does not imply the absence of entanglement between the system (the chain) and reservoirs (the contacts). On the contrary, the entanglement is always there, and it is responsible for the decoherence effect of reservoirs [11].
- [34] Equation (30) also describes the transport of noninteracting Bose particles if one uses the Bose-Einstein distribution instead of the Fermi-Dirac distribution (8).
- [35] A. R. Kolovsky and D. N. Maksimov, Quantum state of the fermionic carriers in a transport channel connecting particle reservoirs, *Condens. Matter* **4**, 85 (2019).
- [36] A. R. Kolovsky, Microscopic models of source and sink for atomtronics, *Phys. Rev. A* **96**, 011601(R) (2017).